Optical properties of the Pb^{2+}-based aggregated phase in a CsCl host crystal: Quantum-confinement effects

M. Nikl,* K. Nitsch, and K. Polak
Institute of Physics, Czech Academy of Sciences, Cukrovarnicka 10, 16200 Prague, Czech Republic

G. P. Pazzi and P. Fabeni
Istituto di Ricerca sulle Onde Elettromagnetiche, Via Panciatichi 64, 50127 Firenze, Italy

D. S. Citrin
Center for Ultrafast Optical Science, The University of Michigan, 2200 Bonisteel Boulevard, Ann Arbor, Michigan 48109-2099

M. Gurioli
European Laboratory for Nonlinear Spectroscopy (LENS), Department of Physics, University of Florence, Largo Enrico Fermi 2, 50125 Firenze, Italy
(Received 14 July 1994)

The quantum-confinement effect is demonstrated in the luminescence of the $CsPbCl_3$-like aggregated phase in Pb^{2+}-doped CsCl single crystals. Namely, microscopic excitonic superradiance is considered to explain the observed picosecond decay kinetics of the aggregated-phase emission band at 420 nm. The low- and high-temperature limits of the temperature dependence of the radiative decay time in the quantum dot are derived and compared with experimental data. Different processes that might influence the observed wavelength and temperature dependence of the observed decay time are discussed.

I. INTRODUCTION

The optical properties of foreign aggregated phases (having the structure of known bulk materials) in crystal or glass matrices are attracting increasing interest in recent years in connection with the study of quantum-confinement effects. [See Refs. 1 – 3, reviews (Refs. 4 and 5), and references therein.] In particular, semiconductor microcrystallites are of interest due to their high radiative efficiency. Pronounced high-energy shifts and substantial broadening of absorption, excitation, and emission spectra[6] have been observed, particularly when at least one dimension of the aggregates is less than about $10a_B$, where a_B is the Bohr radius of the exciton in the equivalent bulk material. This rough limit of aggregate size is further modified by Coulomb and exchange interaction among electron and holes depending on the particular material under consideration. Furthermore, extremely fast components in the decay kinetics have been reported and were explained by microscopic excitonic superradiance in the aggregates.[7] As the typical values of a_B are in the range of a few nanometers, it is necessary to fabricate aggregates in the nanometer size range, in which case the aggregates are usually called nanocrystals, quantum dots (QD), or quantum boxes. Many of the observed phenomena are then explainable as the consequences of the spatial confinement of the exciton motion in the aggregates, which gives rise to the discrete structure of the levels near the bottom of the exciton band with the lowest level shifted to higher energy with respect to the direct excitonic transition in the equivalent bulk material. In addition to the scientific interest in quantum-confinement effects, these phenomena have also attracted attention for applications due to the increased efficiency of excitonic radiative decay in confined systems. Moreover, there is a possible enhancement of the third-order nonlinear optical susceptibility.[8] Even if not in the near future, such materials, therefore, might serve as the basis of an alternative class of solid-state lasers[9] and optoelectronic devices.

The most thoroughly studied systems of this kind are CuCl QD's in NaCl host crystals[10] or in glass matrices[11] and CdS and CdSe (Refs. 12 and 13) QD's in various glass or organic matrices. In addition, a considerable amount of work has been carried out on other material systems. The optical properties of Pb^{2+} ions in alkali halide crystals have been studied for quite some time, primarily due to interest in isolated Pb^{2+} centers in face-centered cubic alkali halides (NaCl structure). It is known that divalent ions tend to aggregate spontaneously in some of these crystal matrices even at room temperature (RT). A quenching procedure is thus currently employed in order to ensure the mutual isolation of the Pb^{2+} ions prior to the optical measurements. The optical properties of the aggregated Pb^{2+} phase were reported only for the Suzuki-like phase (i.e., with irregular structure of aggregates) in KCl:Pb^{2+}.[14] As for the optical properties of Pb^{2+} in body-centered alkali halide crystals (CsCl structure), only a few studies dealing with the absorption[15] and steady-state emission spectra[16,17] of isolated Pb^{2+} centers have been published, and to our knowledge, there is no information available concerning the optical properties of *aggregates* of Pb^{2+} ions in this kind of crystal

0163-1829/95/51(8)/5192(8)/$06.00

©1995 The American Physical Society

lattice.

It should be stressed that the 2+ charge state of Pb is the most stable one in alkali halide crystal lattices at room temperature and that is why we deal with the aggregates based on Pb^{2+} ions. The 1+ charge state of Pb is observed usually only in x- or γ-ray irradiated crystals at sufficiently low temperatures[18] and clusters of Pb^0 atoms have been observed only in rather photosensitive lead halides PbX_2 (X=Cl,Br) after long exposure of UV or x rays.[19]

It is the aim of this paper to report on the optical properties of a system showing the effects of quantum confinement on the exciton motion, namely, the Pb^{2+} aggregated phase in the CsCl host. Its absorption, excitation, and emission spectra are found to be very similar to those of the bulk $CsPbCl_3$ crystal, while the unambiguous influence of the quantum confinement is observed in the decay kinetics. The remainder of this paper is organized as follows. In Sec. II, we discuss the sample preparation and experimental procedures. The results of the cw and time-resolved spectroscopy are presented in Sec. III, while Sec. IV contains a discussion and analysis of these results. We conclude in Sec. V.

II. EXPERIMENT

The crystals of CsCl:Pb (0.01% of $PbCl_2$ in the melt) and $CsPbCl_3$ were grown by the Bridgman technique from chemicals purified by multiple-zone melting.[20] The samples of approximate size $7\times7\times2$ mm were cut from the as-grown crystal and then polished. Thin films of $CsPbCl_3$ on quartz substrates were obtained by evaporation of bulk $CsPbCl_3$ in vacuum from a platinum crucible.

Several types of spectra were obtained employing various experimental setups. Steady-state excitation and emission spectra were measured under excitation by a hydrogen flashlamp on a modified spectrofluorometer 199S manufactured by Edinburgh Instrument (spectral resolution 2.6 nm) and emission spectra with higher resolution (0.25 nm) were obtained by an OMA (EG&G) and excitation by a nitrogen laser. The decay kinetics on the ps time scale were measured by a Hamamatsu streak camera under excitation by the second harmonic of a picosecond dye laser (Antares system). The excitation and emission spectra were corrected for spectral dependence of the excitation energy and spectral response of the monochromator and photomultiplier (OMA head), respectively, to obtain the true profiles. The fluorescence decay times were obtained by deconvoluting the measured signal with the instrument response.

III. EXPERIMENTAL RESULTS

The transmission spectra of the $CsPbCl_3$ thin film and the CsCl:Pb crystal are shown in Fig. 1. The structure in transmission of the as-received CsCl:Pb [Fig. 1(a)] for optical wavelength $\lambda>320$ nm can be erased by quenching (heating at about 400 °C for 30–60 min and fast cooling to RT), as shown in Fig. 1(b), and restored by annealing at temperatures ~200–250 °C for 12–24 h [Fig. 1 (c)]. The position of the lowest absorption peak in Figs. 1(a) and (c) is very close to that of the $CsPbCl_3$ thin film in Fig. 1(d), and can be shifted to the high-energy side of the peak found in the as-received sample by annealing at ~ 200 °C to the quenched samples. Hence, the absorption at $\lambda>320$ nm is clearly connected with the aggregation of Pb^{2+} ions in the CsCl lattice. The steady-state excitation and emission spectra of CsCl:Pb and bulk $CsPbCl_3$ are shown in Fig. 2, and are observed to be to a considerable extent similar for both materials. (λ_m is the wavelength of the emission-line maximum and λ_x is the wavelength of the exciting light.) The intensity of the 420-nm emission band in the CsCl:Pb sample is a monotonically decreasing function of temperature reaching at 180 K about 5–10% of the value at 10 K. The same anomalous high-energy shift (about 7 nm between

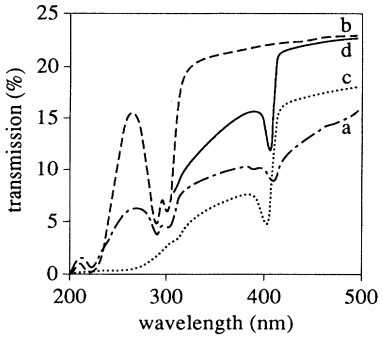

FIG. 1. Transmission spectra of CsCl:Pb and $CsPbCl_3$ thin films at 295 K: (a) as-received CsCl:Pb, (b) CsCl:Pb after the quenching procedure described in the text, (c) CsCl:Pb quenched and annealed at 210 °C for 15 h, (d) $CsPbCl_3$ thin film.

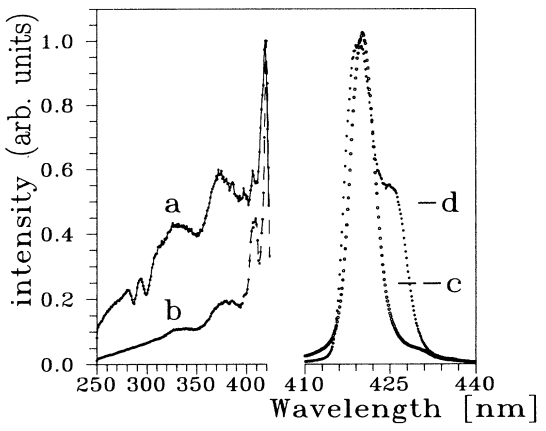

FIG. 2. Excitation and emission spectra of CsCl:Pb and $CsPbCl_3$ single crystals: (a) excitation spectrum of CsCl:Pb, $\lambda_m=418$ nm, $T=4.2$ K; (b) excitation spectrum of $CsPbCl_3$, $\lambda_m=418$ nm, $T=4.2$ K; (c) emission spectrum of CsCl:Pb, $\lambda_x=337$ nm (N_2 laser), $T=10$ K; (d) emission spectrum of $CsPbCl_3$, $\lambda_x=337$ nm (N_2 laser), $T=10$ K.

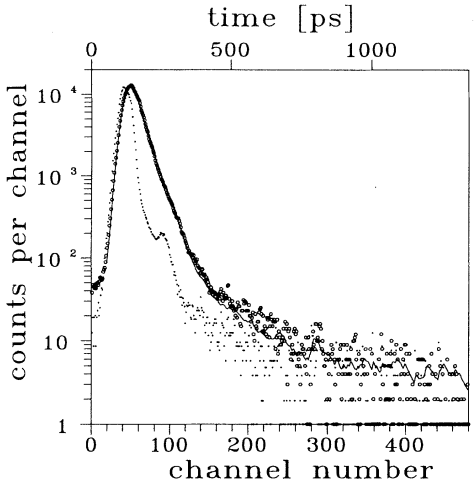

FIG. 3. The decay of CsCl:Pb emission (as-received sample) at the maximum of the band, $\lambda_x = 400$ nm, $\lambda_m = 419$ nm, $T = 10$ K: instrumental response to second harmonic of ps dye laser excitation pulse is given by smaller dots. The solid line is the convolution of the instrumental response with single-exponential function having the decay time 33 ps.

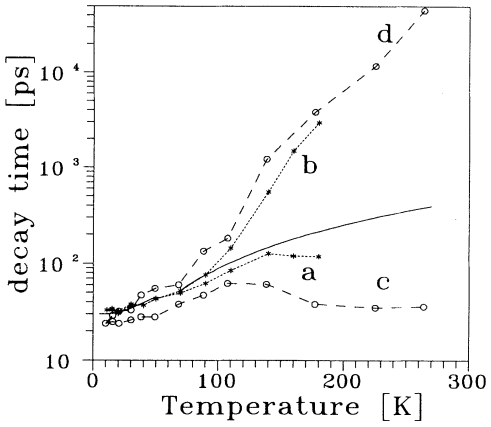

FIG. 5. Temperature dependence of observed decay times, $\lambda_x = 400$ nm. Because of the shift of the emission band with rising temperature (see text), the wavelength was adjusted at every temperature to keep its relative position with respect to the maximum of emission band a constant ($\lambda_m = 419$ nm at 10 K). Curve *a* (*b*) and *c* (*d*) belong to the sample described in caption of Figs. 4(a) and (c), respectively. Curves *c* and *d* were obtained using Eq. (4). See text. The solid line in 5–50 K range is obtained using Eq. (10) with $\Delta E = 2.6$ meV, $\tau_r(0) = 30$ ps. The solid line in 70–270 K range is obtained using Eq. (9) with $\Delta E = 7$ meV, $\tau_r(0) = 30$ ps, and $\epsilon = 1$.

10 and 200 K) of the emission band (with a maximum near 419–420 nm at 4.2 K) with increasing temperature in CsCl:Pb and bulk $CsPbCl_3$ was found, which was earlier reported for $CsPbCl_3$.[21] While the absorption and steady-state emission of the Pb^{2+} aggregated phase in the CsCl host are similar to those of bulk $CsPbCl_3$, their decay kinetics were found to be considerably different. At 10 K three decay times — 0.5, 2.8, and 12 ns — were reported for the decay of the bulk $CsPbCl_3$ emission at 418 nm;[22] however, at 419 nm only single-exponential decay with time constant ~ 30 ps was found in the $CsPbCl_3$-like phase in as-received CsCl:Pb (Fig. 3). The decay curve in the latter case can be fit by a single exponential in the entire wavelength interval examined (406–430 nm at 10 K) with the decay time depending on the wavelength. The general features of this dependence are the same for the samples with different thermal histories (Fig. 4). The temperature dependence of the decay times measured near the emission maximum are shown in Figs. 5(a) and (b) for two different samples.

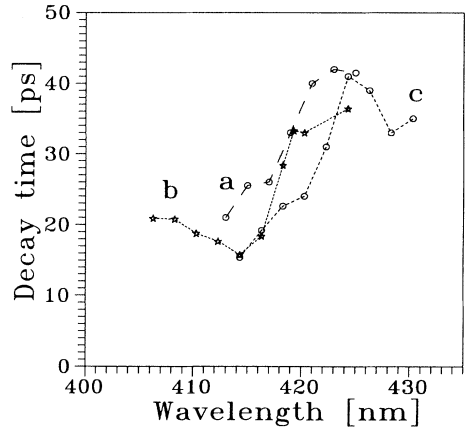

FIG. 4. Wavelength dependence of the decay times obtained at $\lambda_x = 400$ nm, $T = 10$ K: (a) as-received CsCl:Pb [transmission Fig. 1(a)], (b) quenched and annealed CsCl:Pb [transmission Fig. 1(c), 15 h at 210 °C], (c) annealed CsCl:Pb (16 h at 250 °C).

IV. DISCUSSION

It is possible to conclude from the transmission, excitation, and emission spectra presented that the Pb^{2+} aggregated phase in the CsCl host is structurally very similar to the $CsPbCl_3$ structure. We present the following hypothesis for the creation of the $CsPbCl_3$-like structure in Pb^{2+}-doped CsCl (Fig. 6). Two unit cells of the CsCl lattice and Cs^+ ions from the surrounding ones are displayed in Fig. 6(a). The two central Cs^+ ions in the cells are replaced by one Pb^{2+} ion and the charge compensating vacancy in the lower and upper cell, respectively. Let us suppose that the Pb^{2+} ion is delocalized over the two host cation sites in the lower and upper cells passing through the Cl^- plane between the unit cells as shown. During this process, the Pb^{2+} ion has some probability density at the position at the center of Cl^- plane, as mentioned above. This would allow the two original cation sites to become occupied by Cl^- ions displaced from nearby Cl^- sites [Fig. 6(b)]. In such a way, a local structure is created which is very similar to the unit cell of $CsPbCl_3$ [Fig. 6(c)]. The process is

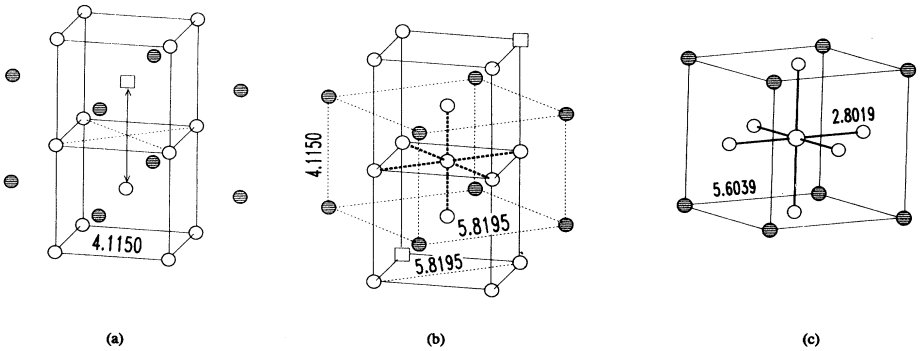

FIG. 6. Mechanism for the formation of the $CsPbCl_3$-like unit cell in the CsCl host doped by Pb^{2+} ions: (a) Pb^{2+} ion in CsCl lattice with a nearby lying charge compensating vacancy, (b) transformation of the local structure towards $CsPbCl_3$-like unit cell, (c) true $CsPbCl_3$ unit cell.

likely to be initiated when several Pb^{2+} ions are close to each other, and the presence of the cation compensating vacancies might make such a Pb^{2+} preaggregate energetically unstable. It is easy to imagine the growth of such a $CsPbCl_3$-like phase in the plane or also in the volume of the CsCl host, because the Cs^+ cation sublattice is almost unchanged and only anion vacancies and/or Cl^- ions in irregular positions can be found at the interface between the foreign phase and host lattice. From another point of view, the slight mismatch in the distances marked in Figs. 6(b) and (c) might be the origin of the observed low-energy shift of the exciton absorption of the $CsPbCl_3$-like phase [Fig. 1(a)] with respect to the absorption peak in the spectrum for the $CsPbCl_3$ thin film [Fig. 1(d)].

The high-energy shift of the excitonic absorption peak in the sample annealed at 210 °C [Fig. 1(c)], with respect to the as-received sample [Fig. 1(a)], can be used as an evidence that, in the former case, the $CsPbCl_3$-like phase aggregates are small enough to confine noticeably the motion of the exciton in the Pb^{2+} sublattice, which has been identified as the Wannier type. This attribution is based on the interpretation of reflection, absorption, and emission spectra of features associated with the Pb^{2+} sublattice of the $CsPbCl_3$ bulk crystal.[21,23] Because of the observed low-energy shift of the exciton absorption in the as-received or heavily annealed (at temperatures about 250 °C) CsCl:Pb samples, with respect to the $CsPbCl_3$ thin film, however, it is difficult to estimate the true quantum-confinement energy, which could be used for the straightforward determination of the aggregate size.

The very fast decay of the $CsPbCl_3$-like phase emission is probably also connected with the confinement of the motion of the exciton in the aggregates. The possibility of strong nonradiative quenching of the emission of the $CsPbCl_3$-like phase (i.e., shortening of observed decay times by this process) can be excluded, because its emission intensity is comparable with that of the bulk $CsPbCl_3$ crystal at 10 K. In particular, we can rule out the dominant role of nonradiative surface states in the decay kinetics, though as we shall see, they may be important in order to explain the details. As already mentioned, the decay rate of the excitonic emission transition can be strongly enhanced compared with the bulk, if the exciton is coherent over the entire volume of the aggregate and the transition dipoles of all the constituent molecules are in phase. The resulting superradiant excitonic decay rate τ_r^{-1} is given by[24]

$$\tau_r^{-1} = 64\left(\frac{R_0}{a_B}\right)^3 \gamma_s, \qquad \gamma_s = \frac{4|\mu_{cv}|^2}{3\hbar\lambda^3}, \tag{1}$$

where R_0 is the radius of the QD (assumed spherical) and μ_{cv} is the matrix element for the interband dipole transition. γ_s is the atomiclike spontaneous-emission rate comparable to the Einstein B coefficient. Because the value of μ_{cv} for $CsPbCl_3$ is not known, we use an atomiclike superradiance model to estimate the number of Pb^{2+} ions in the aggregates. As the Wannier exciton in the Pb^{2+} sublattice is only slightly larger than the $CsPbCl_3$ unit cell ($a_B = 9.8$ Å and the lattice parameter of $CsPbCl_3$ is $a = 5.2$ Å), we can consider the decay rate of the exciton in the $CsPbCl_3$-like aggregate as the volume enhanced decay rate γ_m of the single molecule (unit cell) of $CsPbCl_3$,

$$\tau_r^{-1} = N\gamma_m, \tag{2}$$

where N is the cooperativity number which we can approximately identify with the number of unit cells in the aggregate. The parameter γ_m can be estimated using the radiative decay rates calculated for the KX:Pb^{2+} (X=Cl,Br,I) $^3T_{1u} \rightarrow {}^1A_{1g}$ radiative transition,[25–27] as it is known that the top of valence band and the bottom of the conduction band in $CsPbCl_3$ are associated with the $6s$ and $6p$ functions of Pb^{2+}, respectively,[28] and the first coordination sphere of Pb^{2+} (octahedron of six Cl^- ions) is very similar to those in KX:Pb^{2+} and $CsPbCl_3$. For a realistic estimate it is also necessary to consider the energy separation $E(^3T_{1u} - {}^1T_{1u})$ between the $^3T_{1u}$ and higher-lying $^1T_{1u}$ excited states of Pb^{2+} in the KX matrix. [$E(^3T_{1u} - {}^1T_{1u})$ is decreasing going from the Cl^- to the I^- anion.] The previously mentioned radiative decay rate of the Pb^{2+} ion is determined primarily by the strength of the spin-orbit coupling between the $^1T_{1u}$ and $^3T_{1u}$ levels, which is inversely proportional to $E(^3T_{1u} - {}^1T_{1u})$. The value $E(^3T_{1u} - {}^1T_{1u}) = 0.94$ eV for KI:Pb^{2+} is very close to the energy separation between the two interband Pb^{2+} intraionic s-p transitions (0.95 eV), which can be derived from the absorption spectrum of $CsPbCl_3$ thin films[28] and is closely related to $E(^3T_{1u} - {}^1T_{1u})$ of the isolated Pb^{2+} ion in the KX crys-

tal. Hence, using the values for the radiative decay rates found in KI:Pb,[27] $k_2+k_3=1.1\times10^8$ s^{-1}, Eq. (2) and the value of the observed decay time at the emission maximum at 420 nm in Fig. 4, we find the value of the effective number of $CsPbCl_3$-like unit cells (i.e., approximate number of Pb^{2+} ions) $N\approx250$.

In contrast to the situation found in the decay kinetics of CuCl QD's in the NaCl host[7] or CdS or CdCe QD's in glass matrices,[5] there are virtually no longer decay-time components observed in the $CsPbCl_3$-like QD in the CsCl host (Fig. 3). The long-time components in the other systems have been explained by reabsorption[7] or the existence of extrinsic trap states at the QD-host interface in the glass matrix.[5] Such reabsorption processes are probably inefficient in our case because of the very low concentration of QD's in the sample (estimated QD concentration is in the range of several hundred ppb). Given the present state of knowledge, it is difficult to speculate on the nature of possible trap states at the surface of the $CsPbCl_3$-like QD's; their possible influence will be touched upon below.

A wavelength dependence to the luminescence decay time will arise due to the expected distribution in the size of the aggregates, although quantitative information on this distribution is not yet available. Nevertheless, it is reasonable as a tentative assumption that the emission on the high-energy side of the luminescence band is due to aggregates small enough to produce considerable confinement of the exciton motion. This is supported also by absorption spectra [Fig. 1(c)]. This can explain the relatively flat wavelength dependence of τ_r in Fig. 4(b) for $\lambda<415$ nm. We might also mention other processes, which may further affect the λ dependence of τ_r in this region; at a given temperature the excited states populated in such small aggregates have enhanced probability density near the aggregate boundary and in the host as compared with larger aggregates. Thus, the excited states in the small aggregates are more like the bulk CsCl excitons and, moreover, sample the interface between the aggregate and the host in which case nonradiative (quenching) sites might play a relatively more important role than in larger aggregates.

So far, we have considered only volume states; however, it is well known that surface states may play an important role in luminescence of small QD. Beside extrinsic traps, which serve both as nonradiative centers and centers for donor-acceptor recombination,[29,32] the presence of intrinsic states related to the atoms at the aggregate surface has been reported.[30,31] Excitons bound to such surface states (shallow traps) will be coherent over a region smaller than aggregate volume leading to radiative decay times longer than those of the low-lying QD volume excitons, which is also predicted in Refs. 31 and 32 and, furthermore, can be derived from the dependence of the decay time of the excitons localized at QW width fluctuation on the lateral size of the QW width fluctuation.[33] Such emission is usually situated at the low-energy side of the emission band and, therefore, the increase in the decay time in the region 418–422 nm could be explained in this way. The levelingoff or slight decrease of the decay time above 423 nm is difficult to account for, but it may be connected with the dependence of the surface trap-state coherence volume on the QD size. We have not found any evidence that extrinsic traps are involved in the emission process, because typical decay time of extrinsic trap emission is of the order of several microseconds and no slower components with such decay times have been observed at low energy side of the emission band.

In addition, dephasing times and the degree of thermalization in aggregates of different sizes are expected to be different.[34] This in turn will also lead to a wavelength dependence to the measured decay time.

The temperature dependence of the true excitonic radiative decay time τ_r may be significantly different from that displayed in Figs. 5(a) and (c) because of competing nonradiative processes after thermal equilibrium in the relaxed excited state has been reached. Such processes quench the luminescence and shorten the observed decay time. In this sense, the displayed temperature dependence of τ_r in Figs. 5(a) and (c) provides a lower estimate of the true radiative decay time. To obtain an upper estimate of τ_r, the procedure applied to the analysis of $GaAs/Ga_xAl_{1-x}As$ quantum-well (QW) luminescence[35] can be used, which gives,

$$\tau_r(T,\lambda)=\frac{\tau_L(T,\lambda)}{I_L(T,\lambda)}, \tag{3}$$

where $\tau_L(T,\lambda)$ is the measured decay time and $I_L(T,\lambda)$ is the emission intensity [normalized to $I_L(10\text{ K},\lambda)=1$, assuming quantum efficiency close to 1 at 10 K] derived from the decay-curve measurement using the relation

$$I_L(T,\lambda)=AC\tau_L(T,\lambda), \tag{4}$$

where A is the amplitude of the decay and C is a correction factor taking into account the accumulation time, streak camera sensitivity, and the exciting laser-beam fluctuations. The obtained dependences are given in Figs. 5(b) and (d).

The temperature dependence of the radiative decay time $\tau_r(T)$ in Fig. 5 can be tentatively explained as follows. At sufficiently low temperature, when only the lowest-energy exciton state (energy E_0) is significantly populated, the observed decay time is that characteristic of this level. Moreover, if $k_bT\ll E_n-E_0$, with E_n the energy of higher-lying levels n, then we still have $\tau_r(T)\sim\tau_r(0)$. Now let us consider the states n. The phase of the dipole moment associated with these states has significant spatial variation over the QD, thus leading to partial destructive interference of the fields emitted by the various local dipoles, which in turn leads to decay rates slow compared with that of the lowest-lying level. These considerations are expected to lead to τ_r increasing with T.

Let us put this on quantitative grounds. Assume (i) a thermal population of excitons occupying the various levels,[36] (ii) no dipole-inactive states,[37] and (iii) a cube-shaped QD with infinite barriers to the center-of-mass motion with side length R_0. Moreover, we neglect the possibility of interaggregate cooperativity and, also, the

probable large dielectric mismatch at the aggregate-host interface. The quantized energy levels for the exciton considered as a composite particle are then

$$E_{lmn} = E_0 + \Delta E(l^2 + m^2 + n^2), \tag{5a}$$

$$\Delta E = \frac{\hbar^2 \pi^2}{2MR_0^2}, \tag{5b}$$

where M is the exciton mass. The corresponding wave functions are $\psi(\mathbf{r}) = \phi_l(x)\phi_m(y)\phi_n(z)$ with $\phi_l(x) = \sqrt{2/R_0}\sin x l\pi/R_0$. Neglecting the small but finite photon momentum, the radiative decay rate of $|\psi_{lmn}|^2$ is proportional to the square of the zero–wave-vector component $C_{lmn}(0)$ of ψ_{lmn}, i.e.,

$$C_{lmn}(\mathbf{k}) = \int d^3r\, e^{i\mathbf{k}\cdot\mathbf{r}}\psi_{lmn}(\mathbf{r}). \tag{6}$$

For a thermal population of states the decay rate is[38,39]

$$\tau_r^{-1}(T) = \frac{\sum_{lmn} 2\Gamma_{lmn} e^{-E_{lmn}/k_bT}}{\sum_{lmn} e^{-E_{lmn}/k_bT}}, \tag{7}$$

where

$$2\Gamma_{lmn} = \tau_r^{-1}(0)|C_{lmn}(0)|^2. \tag{8}$$

Γ_{lmn} is the *amplitude* decay rate of state ψ_{lmn} — hence the factor of 2 on the left-hand side of Eq. (8). In the limit $k_bT \gg \Delta E$, the summations in Eq. (7) can be replaced by integrals to give

$$\tau_r(T) \approx \left(\frac{\pi k_bT}{2\epsilon\Delta E}\right)^{3/2} \tau_r(0), \tag{9}$$

where ϵ is a cutoff of the order of unity to guarrantee convergence of the integral in the numerator of Eq. (7). Thus, Eq. (9) predicts a superlinear temperature dependence of $\tau_r(T)$ and is quite different from the two-dimensional case [$\tau_r(T) \propto T$] (Ref. 38) and the one-dimensional case [$\tau_r(T) \propto T^{1/2}$].[40] The result is similar to that predicted for the optically thick bulk GaAs.[41] An attempt was made to fit, using Eq. (9), experimental data for $\tau_r(T)$ for the as-received sample in the temperature range 70–270 K (Fig. 5). Although below 100 K the agreement is satisfactory, at higher temperatures both the lower and upper estimates of $\tau_r(T)$ are substantially different from the theoretical dependence given by Eq. (9). For another estimate of the aggregate size, we may take $\epsilon = 1$, and assume that $\tau_r(90\text{ K})$ lies in the range 60–80 ps using the curves a and b in Fig. 5 at $T = 90$ K (as-received sample) and $\tau_r(0) = 30$ ps. From Eq. (9), we obtain ΔE=7–8 meV. Using the relation between ΔE and R_0 in Eq. (5a), we find the cube edge $R_0 \approx 4$ nm, which contains about 350 $CsPbCl_3$-like unit cells (Pb^{2+} ions), the number being slightly higher than the estimate given above obtained from the cooperativity number. Because of the crude nature of both estimates, it is not possible to discuss in detail this rather small difference; however, one can conclude that each $CsPbCl_3$-like aggregate contains several hundred Pb^{2+} ions for the as-received CsCl:Pb samples.

For $k_bT \ll \Delta E$, we can retain the first terms of the summations in Eq. (3) to give

$$\tau_r(T) \approx \left(1 + 3e^{-3\Delta E/k_bT}\right)\tau_r(0). \tag{10}$$

Due to the noise in the data presented in Fig. 5, it is difficult to fit the low-temperature behaviour to Eq. (10). Nevertheless, an attempt was made (as-received sample) for $\tau_r(0) = 30$ ps, and $\Delta E = 2.6$ meV (solid line in Fig. 5 in the 5–50 K range). However, using the relation between ΔE and R_0 in Eq. (5a) and the size of the $CsPbCl_3$ unit cell, a few thousand Pb^{2+} ions in such aggregate can be expected, which seems to be unrealistic taking into account the rather low nominal concentration of Pb^{2+} ions in the melt. This result also might indicate that strong departures from thermalization take place at low temperatures.

Even if the theoretical prediction given by Eq. (9) is located well between the lower and upper estimates of $\tau_r(T)$ in Fig. 5, serious departures of $\tau_r(T)$ from the thermalization and dephasing models are not excluded, because both models predict $\tau_r(T)$ to be a monotonically increasing function. We comment briefly here on the role of acoustic and optical phonons in determining $\tau_r(T)$. The lattice degrees of freedom associated with the acoustic modes form a quasicontinuum and are, therefore, effective in degrading the temporal[42] and spatial[43] coherence of the macroscopic dipole moment. Thus, as temperature is raised, $\tau_r(T)$ is expected to increase. These effects, however, are small when k_bT exceeds the homogeneous linewidth,[42] which is expected except at the lowest temperatures in Fig. 5. At higher temperatures, the dephasing process is governed mainly by optic phonons.[44] The substantial difference between the lower and upper estimates of $\tau_r(T)$ at higher temperatures is given mainly by the competition between the radiative and nonradiative deexcitation processes,[35] which was taken into account in the simplest way in Eq. (4). However, from the available experimental results it is not possible to estimate the nonradiative losses during the initial electron-hole relaxation preceeding the creation of an exciton. This process is not expected to exert a strong influence on the decay process itself, but rather to reduce the intensity of the luminescence. We believe this kind of nonradiative loss is of some importance, because from the excitation spectrum in Fig. 2, we derive that the efficiency of luminescence under higher-energy (band-band) excitation is considerably smaller than under nearly resonant excitation in the exciton absorption peak. This expectation is supported also by the results obtained theoretically by Benisty *et al.*[34]

Further measurements, primarily high-resolution excitation spectra, temperature dependences of the overall emission under nearly resonant excitation, and the independent determination of the size distribution of the aggregates, are necessary to extract the intrinsic radiative lifetimes of the excitons in the QD's in order to make a close comparison with theoretical predictions.

V. CONCLUSION

The absorption and steady-state excitation and emission spectra of the Pb^{2+}-based aggregated phase in the CsCl host crystal are found to be very similar to those of the $CsPbCl_3$ bulk crystal. The observed picosecond decay kinetics in the former case is ascribed to exciton superradiance due to the spatial coherence of the macroscopic dipole moment associated with radiative transition from the exciton to the crystal ground state in the $CsPbCl_3$-like QD's embedded in the CsCl host. The wavelength and temperature dependences of the decay times observed in the time-resolved spectra are explained based on theoretical and experimental results reported for other QD and QW systems. The most reliable theoretical estimates indicate that the aggregates consist of ~250–350 $CsPbCl_3$-like unit cells, although a less reliable higher estimate was also obtained based upon the low-temperature data. Further, we find that $CsPbCl_3$-like QD's are present already in the as-received CsCl:Pb crystals, and their size can be modified by heat treatment at temperatures in the range 200–250 °C.

ACKNOWLEDGMENTS

One of the authors (M.N.) undertook this work with the support of the ICTP Programme for Training and Research in Italian Laboratories. The financial support of NATO grant under Reference No. HTECH.LG 931435 is also gratefully acknowledged. The work of D.S.C. was supported by the National Science Foundation through the Center for Ultrafast Optical Science under STC PHY 8920108.

* Electronic address: NIKL@FZU.CZ

[1] Al. L. Efros and A. L. Efros, Fiz. Tekh. Poluprovodn. **16**, 1209 (1982) [Sov. Phys. Semicond. **16**, 772 (1982)].
[2] L. E. Brus, J. Chem. Phys. **80**, 4403 (1984).
[3] C. Flytzanis, F. Hache, M. C. Klein, D. Ricard, and P. Roussignol, Prog. Opt. **29**, 323 (1991).
[4] R. Cingolani and R. Rinaldi, Riv. Nuovo Cimento **16**, 1 (1993).
[5] F. Henneberger and J. Puls, in *Optics of Semiconductor Nanostructures*, edited by F. Henneberger, S. Schmitt-Rink, and E. Göbel (Akademie Verlag, Berlin, 1993), pp. 497–545.
[6] T. Itoh, Y. Iwabuchi, and T. Kirihara, Phys. Status Solidi B **146**, 531 (1988).
[7] T. Itoh, M. Furumiya, and T. Ikehara, Solid State Commun. **73**, 271 (1990).
[8] E. Hanamura, Phys. Rev. B **37**, 1273 (1988).
[9] J. Ding, M. Hagerott, T. Ishikara, H. Jeon, and A. V. Nurmikko, Phys. Rev. B **47**, 10 528 (1993).
[10] T. Itoh, Y. Ywabuchi, and M. Kataoka, Phys. Status Solidi B **145**, 567 (1988).
[11] A. I. Ekimov, A. L. Efros, and A. A. Onushchenko, Solid State Commun. **56**, 921 (1985).
[12] Y. Wang and N. Herron, Phys. Rev. B **42**, 7253 (1990).
[13] K. Misawa, S. Nomura, and T. Kobayashi, in *Optics of Semiconductor Nanostructures* (Ref. 5), pp. 447–497.
[14] S. Benci, R. Capelletti, F. Fermi, M. Manfredi, J. Z. Damm, and E. Mugenski, J. Lumin. **18/19**, 341 (1979).
[15] S. Radhakrishna and K. P. Paude, Phys. Rev B **7**, 424 (1973).
[16] N. L. Pathak and S. C. Sen, Indian J. Pure Appl. Phys. **19**, 288 (1975).
[17] S. Radhakrishna, J. Lumin. **12/13**, 409 (1976).
[18] L. E. Nagli, S. V. Djatchenko, Opt. Spektrosk. **61**, 1266 (1986) [Opt. Spectrosc. **61**, 795 (1986)]; Z. Egemberdiev, A. Usarov, S. Zazubovich, Phys. Status Solidi B **164**, 195 (1991).
[19] J. F. Verwey, J. Phys. Chem. Solids **31**, 163 (1970).
[20] K. Nitsch, A. Cihlar, Z. Malkova, M. Rodova, and M. Vanecek, J. Cryst. Growth **131**, 612 (1993).
[21] L. N. Amitin, A. T. Anistratov, and A. I. Kuznetzov, Fiz. Tverd. Tela (Leningrad) **21**, 3535 (1979) [Sov. Phys. Solid State **21**, 2041 (1979)].
[22] M. Nikl, E. Mihokova, K. Nitsch, K. Polak, M. Rodova, G. P. Pazzi, P. Fabeni, and M. Gurioli, Chem. Phys. Lett. **220**, 14 (1994).
[23] I. P. Pashchuk, N. S. Pidzyrailo, and M. G. Macko, Fiz. Tverd. Tela (Leningrad) **23**, 2162 (1981) [Sov. Phys. Solid State **23**, 1263 (1981)].
[24] E. Hanamura, Phys. Rev B **38**, 1228 (1988).
[25] J. G. Kang, F. Cusso, T. F. Belliveau, and D. J. Simkin, J. Phys. C **18**, 4753 (1985).
[26] K. Polak, M. Nikl, and E. Mihokova, J. Lumin. **54**, 189 (1992).
[27] E. Mihokova, M. Nikl, K. Polak, and K. Nitsch, J. Phys. Condens. Matter **6**, 293 (1994).
[28] K. Heidrich, H. Kunzel, and J. Treusch, Solid State Commun. **25**, 887 (1978).
[29] N. Chesnoy, T. D. Harris, R. Hull, and L. E. Brus, J. Phys. Chem. **90**, 3393 (1984).
[30] M. G. Bavendi, P. J. Carrol, W. L. Willson, and L. E. Brus, J. Phys. Chem. **96**, 946 (1992).
[31] F. Hache, M. C. Klein, D. Richard, and C. Flytzanis, J. Opt. Soc. Am. B **8**, 1802 (1991).
[32] L. Brus, IEEE J. Quantum Electron. **QE-22**, 1909 (1986).
[33] D. S. Citrin, Phys. Rev. B **47**, 3832 (1993).
[34] H. Benisty, C. M. Sotomayor-Torres, and C. Weisbuch, Phys. Rev. B **44**, 10 945 (1991).
[35] M. Gurioli, A. Vinattieri, M. Colocci, C. Deparis, J. Massies, G. Neu, A. Bosacchi, and S. Franchi, Phys. Rev. B **44**, 3115 (1991).
[36] The reader is cautioned that there is a debate whether thermalization is in fact achievable due to a possible phonon bottleneck preventing energy relaxation. See Ref. 34.
[37] Provided thermalization is satisfied or the spin relaxation time is sufficiently fast, this assumption is irrelevant.
[38] L. C. Andreani, F. Tassone, and F. Bassani, Solid State Commun. **77**, 641 (1991).
[39] H. Fidder, J. Knoester, and D. A. Wiersma, Chem. Phys. Lett. **171**, 529 (1990); T. Takagahara, Phys. Rev. B **47**,

16 639 (1993).
[40] D. S. Citrin, Phys. Rev. Lett. **69**, 3393 (1992).
[41] G. W. Hooft, W. A. van der Poel, L. W. Molenkamp, and C. T. Foxon, Phys. Rev. B **35**, 8281 (1987).
[42] D. S. Citrin, Solid State Commun. **84**, 281 (1992); Phys. Rev. B **47**, 3832 (1993).
[43] F. C. Spano, J. R. Kuklinski, and S. Mukamel, Phys. Rev. Lett. **65**, 311 (1990).
[44] D. S. Kim, J. Shah, J. E. Cunningham, T. C. Damen, W. Schäfer, M. Hartmann, and S. Schmitt-Rink, Phys. Rev. Lett. **68**, 1006 (1992).